enhances IgG and IgM production and induces secretion of IgE [F. Rousset, E. Garcia, J. Banchereau, unpublished data].
9. Established cell lines were found to die out after 10 weeks for presently unexplained reasons. Induction of B cell proliferation with immobilized anti-CD40 turned out to be a very constant feature over 30 months and more than 30 B cell lines have been established from various sources. More than 100 experiments with 60 different tonsils, 18 experiments with cord blood, 30 experiments with peripheral blood, and 18 experiments with four different spleens have shown proliferation of B cells with anti-CD40 + CDw32 L cells.
10. Z. Darzynkiewicz, F. Traganos, M. R. Melamed, *Cytometry* **1**, 98 (1980).
11. Y. J. Liu *et al.*, *Nature* **342**, 929 (1989).
12. T. Stamenkovic, *et al.*, *EMBO. J.* **8**, 1403 (1989).
13. H. Loetscher *et al.*, *Cell* **61**, 351 (1990); T. J. Schall *et al.*, *ibid.*, p. 361; C. A. Smith *et al.*, *Science* **248**, 1019 (1990).
14. T. Defrance *et al.*, *J. Immunol.* **139**, 1135 (1987).
15. B. M. Reedman and G. Klein, *Int. J. Cancer* **11**, 499 (1973).
16. I. Lefkovits and H. Waldmann, in *Limiting Dilution Analysis of Cells of the Immune System* (Cambridge Univ. Press, New York, 1985), p. 81.
17. We thank K. Moore (DNAX) for providing CDw32 L cells and continuous interest through the present study, G. Lenoir for testing EBNA protein expression, J. M. Seigneurin for testing EBNA2 expression by polymerase chain reaction, A. M. Manel for karyotype analysis, A. Waitz, R. Callard, and H. Martinez-Valdez for reading the manuscript, and N. Courbière for expert editorial assistance. A.V. was supported by the Mérieux Fondation.

29 May 1990; accepted 16 October 1990

Expression cDNA Cloning of the KGF Receptor by Creation of a Transforming Autocrine Loop

TORU MIKI, TIMOTHY P. FLEMING, DONALD P. BOTTARO, JEFFREY S. RUBIN, DINA RON, STUART A. AARONSON

An expression cloning strategy was devised to isolate the keratinocyte growth factor (KGF) receptor complementary DNA. NIH/3T3 fibroblasts, which secrete this epithelial cell–specific mitogen, were transfected with a keratinocyte expression complementary DNA library. Among several transformed foci identified, one demonstrated the acquisition of specific high-affinity KGF binding sites. The pattern of binding competition by related fibroblast growth factors (FGFs) indicated that this receptor had high affinity for acidic FGF as well as KGF. The rescued 4.2-kilobase complementary DNA was shown to encode a predicted membrane-spanning tyrosine kinase related to but distinct from the basic FGF receptor. This expression cloning approach may be generally applicable to the isolation of genes that constitute limiting steps in mitogenic signaling pathways.

GROWTH FACTOR SIGNALING PATHways have critical roles in normal development and in the genetic alterations associated with the neoplastic process (*1*). The isolation of cDNAs for important components of these pathways has generally involved difficult and time-consuming protein isolation and purification. Cloning methods based on transient expression assays (*2*) also require laborious screening procedures, sensitive biologic assays, or the availability of immunologic reagents capable of recognizing the gene product. In certain cases, naive cells have been shown to inherently express all of the necessary intracellular components required for effective mitogenic signaling if a given receptor can be artificially expressed and the appropriate ligand can be provided (*3*). Moreover, completion of an autocrine loop involving expression of a ligand and its receptor by the same cell can be associated with uncontrolled proliferation and malignant transformation (*4*). We reasoned that the stable ectopic expression of cDNA clones might result in the transformed phenotype if an autocrine loop were created, for example, by introduction of a growth factor receptor cDNA into cells expressing only its ligand. We have described a directional cDNA library expression vector that has all of the properties likely to be useful in testing this approach, including the capacity for plasmid rescue, a selectable marker, and a strong constitutive promoter (*5*). The ability of the method to synthesize long cDNAs with complete coding sequences has also been shown (*6*).

Keratinocyte growth factor (KGF) has potent mitogenic activity for a wide variety of epithelial cells but lacks detectable activity on fibroblasts or endothelial cells (*7*). Its synthesis by stromal fibroblasts in a large number of epithelial tissues has suggested that KGF is an important paracrine mediator of normal epithelial cell proliferation (*8*). Studies have further indicated specific KGF binding to keratinocytes but not fibroblasts (*9*). Thus, we sought to test the feasibility of our expression cloning strategy in the search to identify and functionally clone the receptor for this new growth factor.

We prepared a cDNA library (4.5×10^6 independent clones) from BALB/MK epidermal keratinocytes (*10*) in an improved vector, λpCEV27 (*11*), and transfected NIH/3T3 mouse embryo fibroblasts (*12*), which synthesize KGF (*13*). We detected 15 transformed foci among a total of 100 individual cultures. Each was shown to be resistant to G418, indicating that it contained integrated vector sequences. Three representative transformants were chosen for more detailed characterization based on differences in their morphologies. Several plasmids were isolated from each transformant after plasmid rescue (*14*). A single cDNA clone rescued from each transformant was found to possess high-titered transforming activity ranging from 10^3 to 10^4 focus-forming units per nanomole of DNA. Transfectants induced by the individual plasmids containing these epithelial cell-transforming cDNAs (designated *ect*1, *ect*2, and *ect*3) were used in subsequent analyses.

To investigate the possibility that any of the three genes might encode the KGF

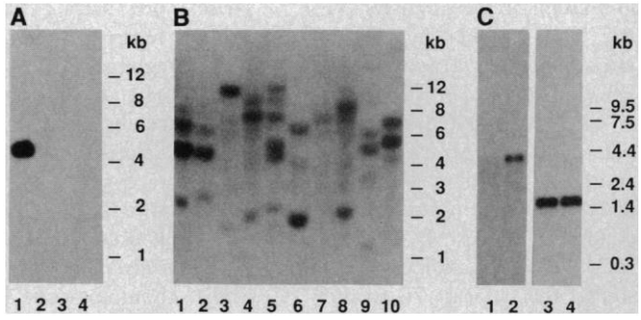

Fig. 1. Genomic analysis of *ect*1 DNA and comparative RNA expression. (**A**) Southern analysis of the Sal I–digested DNAs from NIH/3T3 and its transformants. The blot was probed (*28*) with the entire *ect*1 cDNA insert. Lane 1, NIH/*ect*1; lane 2, NIH/*ect*2; lane 3, NIH/*ect*3; lane 4, NIH/3T3. (**B**) Southern analysis of Eco RI–digested DNAs of different animal species (Clontech Labs, Inc.). The blot was probed (*28*) with the 5′-half of the *ect*1 cDNA insert (Fig. 2B) and washed under reduced stringency conditions. Lane 1, human; lane 2, rhesus monkey; lane 3, mink; lane 4, cat; lane 5, mouse; lane 6, cow; lane 7, chicken; lane 8, dog; lane 9, guinea pig; lane 10, pig. (**C**) Northern analysis of NIH/3T3 and BALB/MK RNA. The blot was probed (*29*) with the 5′-half of the *ect*1 cDNA (lanes 1 and 2) or a β-actin cDNA (lanes 3 and 4) and washed under stringent conditions. Lanes 1 and 3, NIH/3T3; lanes 2 and 4, BALB/MK.

Laboratory of Cellular and Molecular Biology, National Cancer Institute, Bethesda, MD 20892.

receptor, we performed binding studies with recombinant ^{125}I-labeled KGF. BALB/MK cells showed specific high affinity binding of ^{125}I-labeled KGF, which was not observed when NIH/3T3 cells were used. Expression of the *ect*1 gene by NIH/3T3 cells resulted in the acquisition of 3.5-fold more ^{125}I-labeled KGF binding sites than BALB/MK cells. Under the same conditions, control NIH/3T3 as well as transfectants containing either *ect*2 or *ect*3 did not bind the labeled growth factor. These results suggested that *ect*1 encoded the KGF receptor (KGFR), whose introduction into NIH/3T3 cells had completed an autocrine transforming loop.

To characterize *ect*1, we used the transforming 4.2-kb cDNA released by Sal I digestion as a molecular probe to hybridize Sal I–digested genomic DNAs. Since Sal I is an infrequent cutter, the large genomic DNA fragments migrated near the origin of the gel. The expected 4.2-kb DNA fragment was detected in the *ect*1 transformant (Fig. 1A), but neither NIH/3T3 nor the other transfectants showed evidence of a Sal I fragment hybridized by the cDNA insert. These results further argued that the *ect*2 and *ect*3 represented independent transforming genes. When Eco RI was used to cleave normal mouse DNA, we observed several distinct *ect*1-hybridizing DNA fragments, which reflected endogenous *ect*1 sequences or closely related genes (Fig. 1B). These *ect*1-related sequences were also observed in the DNAs of other species analyzed, including human, indicating its high degree of conservation in vertebrate evolution. A single *ect*1 transcript of around 4.2 kb was observed in BALB/MK cells (Fig. 1C). Thus, our cDNA clone represented essentially the complete *ect*1 transcript. In NIH/3T3 cells, a transcript of comparable size was only faintly detactable under stringent hybridization conditions. Thus, if this transcript were to represent *ect*1 rather than a related gene, its expression was markedly lower in fibroblasts as compared to epithelial cells.

Fig. 3. Competition of KGF (□), aFGF (○), and bFGF (△) for ^{125}I-labeled KGF binding (*31*) on BALB/MK cells (**A**) and NIH/*ect*1 cells (**B**). Binding assays were performed as described previously (*9*).

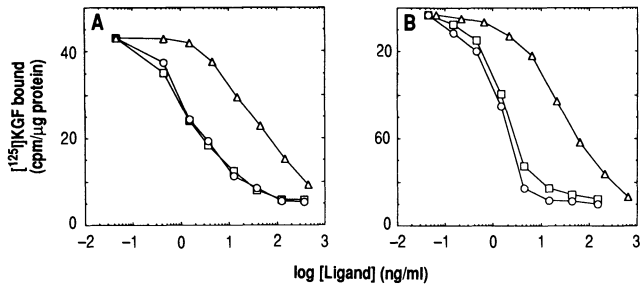

Nucleotide sequence analysis of the 4.2-kb *ect*1 cDNA revealed a long open reading frame of 2235 nucleotides (nucleotide position 562 to 2796). Two methionine codons were found at nucleotide positions 619 and 676, respectively. The second methionine codon matched the Kozak's consensus for a translational initiator sequence (A/GCCATGG) (*15*). Moreover, it was followed by a characteristic signal sequence of 21 residues, 10 of which were identical to those of the putative signal peptide of the mouse basic FGF (bFGF) receptor (*16, 17*). Thus, it seems likely that the second ATG is the authentic initiation codon. If so, the receptor polypeptide would comprise 707 amino acids with a predicted size of 82.5-kD (Fig. 2A).

The amino acid sequence predicted a transmembrane tyrosine kinase closely related to the mouse bFGF receptor (bFGFR). The percent similarity between both proteins is shown in Fig. 2B. The putative KGFR extracellular portion contained two immunoglobulin (Ig)-like domains, exhibiting 77% and 60% similarity with the Ig-like domains 2 and 3, respectively, of the mouse bFGFR. Studies have revealed a variant form of the bFGFR, in which the extracellular domain also contains only these two corresponding Ig-like domains (*17*). The sequence NH_2-terminal to the first Ig-like domain of the KGFR was 63 residues long in comparison to 88 residues found in the shorter form of the mouse bFGFR. Both chicken and mouse bFGFRs contain a stretch of eight consecutive acidic residues between the first and second Ig-like domains (*16–18*). The KGFR lacked such an acidic amino acid domain (Fig. 2B).

The kinase domain of the KGFR was 90% related to the bFGFR tyrosine kinase (Fig. 2B). The central core of the catalytic domain was flanked by a relatively long juxtamembrane sequence, and the tyrosine kinase domain was split by a short insert of 14 residues, similar to that observed in mouse, chicken, and human bFGF receptors (*16–19*). Hanafusa and co-workers isolated a partial cDNA for a tyrosine kinase gene, designated *bek*, by bacterial expression cloning with phosphotyrosine antibodies (*20*). The reported sequence of *bek* was identical to the KGFR in the tyrosine kinase domain (Fig. 2B).

Scatchard analysis of ^{125}I-labeled KGF binding to the NIH/*ect*1 transfectant revealed expression of two similar high-affinity receptor populations. Out of a total of ~3.8 × 10^5 sites per cell, 40% displayed a dissociation constant (K_d) of 180 pM and the remaining 60% showed a K_d of 480 pM (*21*). These values are comparable to the high-affinity KGF binding sites displayed by BALB/MK cells (*9*). The pattern of KGF

A

```
1   MVSWGRFICLVLVTMATLSLARPSFSLVEDTTLEPEGAPYWTNTEKMEKRLHAVPAANTVKFRCPAGGNPTPTMRWLKNG
81  KEFKQEHRIGGYKVRNQHWSLIMESVVPSDKGNYTCLVENEYGSINHTYHLDVVERSPHRPILQAGLPANASTVVGGDVE
161 FVCKVYSDAQPHIQWIKHVEKNGSKYGPDGLPYLKVLKHSGINSSNAEVLALFNVTEMDAGEYICKVSNYIGQANQSAWL
241 TVLPKQQAPVREKEITASPDYLEIAIYCIGVFLIACMVVTVIFCRMKTTTKKPDFSSQPAVHKLTKRIPLRRQVTVSAES
321 SSSMNSNTPLVRITTRLSSTADTPMLAGVSEYELPEDPKWEFPRDKLTLGKPLGEGCFGQVVMAEAVGIDKDKPKEAVTV
401 AVKMLKDDATEKDLSDLVSEMEMMKMIGKHKNIINLLGACTQDGPLYVIVEYASKGNLREYLRARRPPGMEYSYDINRVP
481 EEQMTFKDLVSCTYQLARGMEYLASQKCIHRDLAARNVLVTENNVMKIADFGLARDINNIDYYKKTTNGRLPVKWMAPEA
561 LFDRVYTHQSDVWSFGVLMWEIFTLGGSPYPGIPVEELFKLLKEGHRMDKPTNCTNELYMMMRDCWHAVPSQRPTFKQLV
641 EDLDRILTLTTNEEYLDLTQPLEQYSPSYPDTRSSCSSGDDSVFSPDPMPYEPCLPQYPHINGSVKT
```

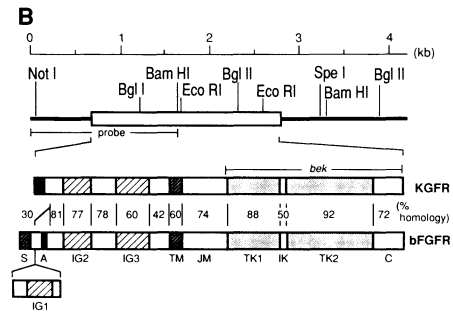

Fig. 2. Primary structure of the KGF receptor. (**A**) Amino acid sequence deduced from the coding region of the KGF receptor cDNA. Amino acids are numbered from the putative initiation site of translation. Potential sites of N-linked glycosylation are underlined. The potential signal peptide and transmembrane domains are boxed. The interkinase domain is shown by underlined italic letters. Glycine residues considered to be involved in ATP (adenosine triphosphate) binding are indicated by asterisks. Cysteine residues delimit two Ig-like domains in the extracellular portion of the molecule are shown by bold face. Nucleotide sequence was determined by the chain termination method (*30*). (**B**) Structural comparison of the predicted KGF and bFGF receptors. The region used as a probe for Southern and Northern analysis (Fig. 1, B and C) is indicated. The region homologous to the published *bek* sequence (*20*) is also shown. The schematic structure of the KGF receptor is shown below the restriction map of the cDNA clone. Amino acid sequence similarities with the smaller and larger bFGF receptor variants are indicated. S, signal peptide; A, acidic region; IG1, IG2, and IG3, Ig-like domains; TM, transmembrane domain; JM, juxtamembrane domain; TK1 and TK2, tyrosine kinase domains; IK, interkinase domain; C, COOH-terminus domain.

and FGF competition for ^{125}I-labeled KGF binding to NIH/*ect*1 cells was also very similar to that observed with BALB/MK cells (Fig. 3). Although maximum ^{125}I-labeled KGF binding to NIH/*ect*1 cells was 3.5 times higher than to BALB/MK, there was 50% displacement by 2 ng/ml of either KGF or acidic FGF (aFGF) with each cell type. Similarly, both cells showed 15 times less efficient competition by bFGF for bound ^{125}I-labeled KGF. Thus, the cloned KGFR exhibited the characteristic pattern of KGF and FGF competition displayed by BALB/MK cells, which suggests the KGFR is a high-affinity receptor for aFGF as well as KGF.

When ^{125}I-labeled KGF is cross-linked to its receptors on BALB/MK cells, two protein species of 162- and 137-kD have been observed (*9*). Taking into account the size of KGF itself, we have estimated the cross-linked receptors to be around 140- and 115-kD, respectively. When ^{125}I-labeled KGF cross-linking was performed with NIH/*ect*1 cells, we observed a single species corresponding in size to the smaller, 137-kD complex in BALB/MK cells (Fig. 4A). Moreover, detection of this band was specifically and efficiently blocked by unlabeled KGF. When glycosylation is considered, the size of the KGFR predicted by sequence analysis corresponds reasonably well with the corrected size (115 kD) of the cross-linked KGFR in the *ect*1 transfectant.

To further examine the functional nature of the KGFR expressed in NIH/*ect*1 cells, we investigated its capacity to induce tyrosine phosphorylation of cellular proteins. NIH/3T3 or NIH/*ect*1 cells were exposed to KGF for 10 min and cell lysates were subjected to immunoprecipitation and immunoblotting analysis with antibody to phosphotyrosine (anti-Ptyr). NIH/*ect*1 cells contained several tyrosine-phosphorylated proteins that were not detectable in control or KGF-stimulated NIH/3T3 cells (Fig. 4B). Addition of KGF to NIH/*ect*1 cells resulted in the detection or increased tyrosine phosphorylation of several putative substrates. These included p55, p65, p90, p115, p150, and p190. These findings established that the KGFR was enzymatically activated in response to KGF. Previous studies have indicated that similar-size proteins are phosphorylated in response to KGF triggering of BALB/MK cells (*9*). Moreover, the 115-kD phosphoprotein matched the corrected size of the KGFR cross-linked by ^{125}I-labeled KGF.

Our expression cloning of the KGFR was based on its transforming activity for NIH/3T3 cells that synthesize KGF. Thus, its detection could reflect activation of an autocrine loop involving KGF and the normal receptor. Alternatively, the cDNA might have been fortuitously detected as a constitutively activated KGFR mutant. Suramin, which interferes with ligand-receptor interactions (*22*), inhibited DNA synthesis of KGFR transfectants. We also observed specific inhibition of proliferation of such cells in response to a KGF monoclonal antibody, which neutralizes KGF mitogenic activity (*23*). Together these findings argue that induction of the transformed phenotype resulted from autocrine KGF stimulation of an ectopically expressed normal KGFR cDNA.

We isolated at least two additional genes from our epithelial cell cDNA expression library with transforming activity for fibroblasts. Their relation to growth signaling pathways awaits further characterization. Given the normal juxtaposition of other cell types and stromal fibroblasts in vivo and their likely paracrine interactions, it may be possible to identify additional growth factors or their receptors by transfecting NIH/3T3 cells with expression libraries from these other sources. It is also conceivable that introduction of tissue-specific genes encoding downstream targets of growth factor receptor signaling might complete an autocrine loop in a recipient cell if it had a critical regulatory role. Thus, our expression cloning strategy may aid in the identification and isolation of genes for such intracellular components of mitogenic signaling pathways.

There have been reports concerning human or avian cDNAs closely related to the KGFR (*24–26*). The external portions of *bek* (human) and *cek*3 (chicken) proteins contain three Ig-like domains (*24, 25*). These molecules also differ from the KGFR in that each contains an acidic region and is completely divergent in the COOH-terminal half of its third Ig-like domain from the KGFR. Binding studies with the three Ig-like domain human *bek* variant have indicated similar high affinities for aFGF and bFGF (*24*). Since the affinity of the KGFR for aFGF was substantially higher than for bFGF, differences in FGF binding by these receptor molecules must relate to these regions of divergence. In BALB/MK cells, we detected a higher molecular weight KGF–cross-linked species, corresponding in size to the three Ig-like domain *bek* variant (*9*). Whether it represents this variant or the product of a distinct gene remains to be determined. A gene, designated K-*sam*, was identified as an amplified sequence in a human stomach carcinoma (*26*). A cDNA clone corresponding to one of the overexpressed K-*sam* transcripts predicts a two Ig-like domain *bek* variant, whose Ig-like domains correspond to those of the KGFR. However, it differs in that it contains an acidic region and may be truncated at its COOH-terminus as well (*26*). These molecules likely reflect alternative transcripts of the same gene, as has also been suggested for two and three Ig-like domain forms of the bFGFR (*27*).

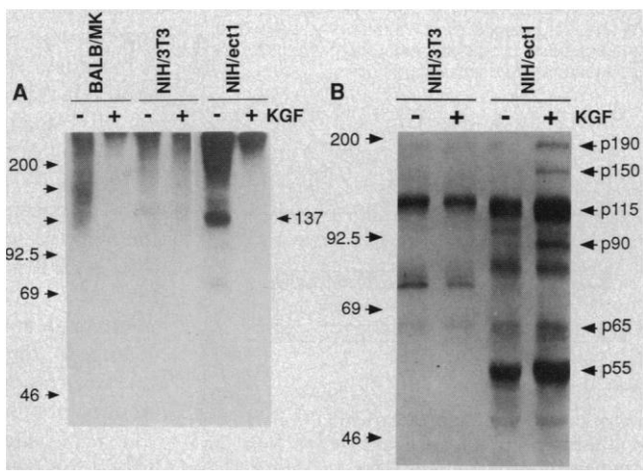

Fig. 4. Analysis of the KGF receptor expressed in NIH/3T3 cells. (**A**) Covalent affinity cross-linking of ^{125}I-labeled KGF to BALB/MK, NIH/3T3, and NIH/*ect*1 cultures. The left and center panels of this autoradiogram were exposed to Kodak XAR film for 72 hours at −70°C; the right panel is an 18-hour exposure of the same autoradiogram. The second lane (labeled +) for each cell type shows cross-linking performed in the presence of excess unlabeled KGF. Molecular weight markers ($\times 10^{-3}$) are indicated on the left; the positions of ^{125}I-labeled KGF–cross-linked complexes are indicated by arrows. Cross-linking was carried out as described previously (*9*). (**B**) Autoradiogram of phosphotyrosyl-proteins from intact NIH/3T3 and NIH/*ect*1 cells before and after treatment with KGF. Molecular weight markers are indicated on the left; the estimated molecular weights of proteins displaying KGF-stimulated phosphorylation on tyrosine are shown at right. Analysis of phosphoproteins was performed as described previously (*9*).

REFERENCES AND NOTES

1. G. Guroff, in *Oncogenes, Genes, and Growth Factors*, G. Block and J. Marsh, Eds. (Wiley-Interscience, New York, 1987), pp. 191–224; P. Kahn and T. Graf, Eds., *Oncogenes and Growth Control* (Springer-Verlag, New York, 1986).
2. H. Okayama and P. Berg, *Mol. Cell. Biol.* **3**, 280 (1983); A. Aruffo and B. Seed, *Proc. Natl. Acad. Sci. U.S.A.* **84**, 8573 (1987).
3. J. H. Pierce *et al.*, *Science* **239**, 628 (1988).
4. A. Gazit *et al.*, *Cell* **39**, 89 (1984); D. Julius *et al.*, *Science* **244**, 1057 (1989).
5. T. Miki *et al.*, *Gene* **83**, 137 (1989).

6. T. Matsui *et al.*, *Science* **243**, 800 (1989); M. H. Kraus *et al.*, *Proc. Natl. Acad. Sci. U.S.A.* **86**, 9193 (1989); G. D. Kruh *et al.*, *ibid.* **87**, 5802 (1990).
7. J. S. Rubin *et al.*, *Proc. Natl. Acad. Sci. U.S.A.* **86**, 802 (1989).
8. P. W. Finch *et al.*, *Science* **245**, 752 (1989).
9. D. P. Bottaro *et al.*, *J. Biol. Chem.* **265**, 12767 (1990).
10. B. E. Weissman and S. A. Aaronson, *Cell* **32**, 599 (1983).
11. T. Miki, unpublished data.
12. J. L. Jainchill, S. A. Aaronson, G. J. Todaro, *J. Virol.* **4**, 549 (1969).
13. J. S. Rubin, unpublished data.
14. Genomic DNA from each transformant was cleaved by one of the infrequent cutters that can release the plasmids containing cDNA inserts. Digested DNA was ligated under diluted conditions and used to transform bacterial-competent cells. Plasmids were isolated from ampicillin- and kanamycin-resistant transformants and used to transfect NIH/3T3 cells to examine for focus formation. The *ect*1 plasmid was rescued by Xho I, while the *ect*2 and *ect*3 plasmids were rescued by Not I digestion.
15. M. Kozak, *Nucleic Acids Res.* **5**, 8125 (1987).
16. A. Safran *et al.*, *Oncogene* **5**, 635 (1990).
17. H. H. Reid, A. F. Wilks, O. Bernard, *Proc. Natl. Acad. Sci. U.S.A.* **87**, 1596 (1990); A. Mansukuhani, D. Moscatelli, D. Talarico, V. Levytska, C. Basilico, *ibid.*, p. 4378.
18. P. L. Lee, D. E. Johnson, L. S. Cousens, V. A. Fried, L. T. Williams, *Science* **245**, 57 (1989); E. B. Pasquale and S. J. Singer, *Proc. Natl. Acad. Sci. U.S.A.* **86**, 8722 (1989).
19. M. Ruta *et al.*, *Oncogene* **3**, 9 (1988); M. Ruta *et al.*, *Proc. Natl. Acad. Sci. U.S.A.* **86**, 5449 (1989).
20. S. Kornbluth, K. E. Paulson, H. Hanafusa, *Mol. Cell. Biol.* **8**, 5541 (1988).
21. D. P. Bottaro, unpublished data.
22. C. Betsholtz, A. Johnsson, C.-H. Heldin, B. Westermark, *Proc. Natl. Acad. Sci. U.S.A.* **83**, 6440 (1986); T. P. Fleming *et al.*, *ibid.* **86**, 8063 (1989).
23. J. S. Rubin, unpublished data.
24. C. A. Dionne *et al.*, *EMBO J.* **9**, 2685 (1990).
25. E. B. Pasquale, *Proc. Natl. Acad. Sci. U.S.A.* **87**, 5812 (1990).
26. Y. Hattori *et al.*, *ibid.*, p. 5983.
27. D. E. Johnson, P. L. Lee, J. Lu, L. T. Williams, *Mol. Cell. Biol.* **10**, 4728 (1990).
28. DNA (10 μg) was digested by Sal I (Fig. 1A) or Eco RI (Fig. 1B), fractionated by agarose gel electrophoresis, and transferred to a nylon-supported nitrocellulose paper (Nitrocellulose-GTG, FMC Corp.). The blot in Fig. 1A was hybridized with the ^{32}P-labeled entire *ect*1 insert at 42°C and washed at 65°C in 0.1× saline sodium citrate (SSC), while the blot in Fig. 1B was hybridized with the ^{32}P-labeled 5′-*ect*1 probe (Fig. 2B) at 37°C and washed at 55°C in 0.1× SSC. Hybridization experiments were performed at the indicated temperature in a solution containing 50% formamide, 5× SSC, 2.5× Denhardt solution, 7 mM tris-HCl (pH 7.5), denatured calf thymus DNA (0.1 mg/ml), and tRNA (0.1 mg/ml). Location of DNA markers (BRL, Gaithersburg, MD) is indicated in kilobases.
29. Polyadenylated RNA preparations (5 μg each) were fractionated by formaldehyde gel, transferred to Nitrocellulose-GTG, and hybridized with the 5′-*ect*1 probe (Fig. 1C, lanes 1 and 2). After autoradiography, the filter was boiled to remove the probe and then hybridized with a β-actin probe (lanes 3 and 4). Location of markers (BRL, Gaithersburg, MD) is indicated in kilobases.
30. F. Sanger, S. Nicklen, A. R. Coulson, *Proc. Natl. Acad. Sci. U.S.A.* **74**, 5463 (1977).
31. To control for the quality of the ^{125}I-labeled and unlabeled ligands, we tested each and all were mitogenic at picomolar concentrations on either BALB/MK (aFGF and KGF) or NIH/3T3 (aFGF and bFGF). As previously reported (*9*), the aFGF and bFGF preparations competed with similar efficiency for ^{125}I-labeled aFGF binding to NIH/3T3 cells.
32. We thank J. Ong, J. Artrip, M. Moore, and C. Smith for excellent technical support; P. W. Finch and M. H. Kraus for materials; and S. R. Tronick for computer analysis.

18 June 1990; accepted 2 November 1990

Generation of Calcium Oscillations in Fibroblasts by Positive Feedback Between Calcium and IP_3

ALEC T. HAROOTUNIAN, JOSEPH P. Y. KAO,* SUMAN PARANJAPE, ROGER Y. TSIEN†

A wide variety of nonexcitable cells generate repetitive transient increases in cytosolic calcium ion concentration ($[Ca^{2+}]_i$) when stimulated with agonists that engage the phosphoinositide signalling pathway. Current theories regarding the mechanisms of oscillation disagree on whether Ca^{2+} inhibits or stimulates its own release from internal stores and whether inositol 1,4,5-trisphosphate (IP_3) and diacylglycerol (DG) also undergo oscillations linked to the Ca^{2+} spikes. In this study, Ca^{2+} was found to stimulate its own release in REF52 fibroblasts primed by mitogens plus depolarization. However, unlike Ca^{2+} release in muscle and nerve cells, this amplification was insensitive to caffeine or ryanodine and required hormone receptor occupancy and functional IP_3 receptors. Oscillations in $[Ca^{2+}]_i$ were accompanied by oscillations in IP_3 concentration but did not require functional protein kinase C. Therefore, the dominant feedback mechanism in this cell type appears to be Ca^{2+} stimulation of phospholipase C once this enzyme has been activated by hormone receptors.

MANY NONEXCITABLE CELLS exhibit periodic increases (spikes) in the concentration of cytosolic free calcium ($[Ca^{2+}]_i$) when stimulated with hormones or growth factors (*1*). The biochemical mechanism and physiological significance of these $[Ca^{2+}]_i$ oscillations are still highly controversial. At least four classes of generating mechanisms have been proposed (Table 1). These can be distinguished by whether inositol 1,4,5-trisphosphate concentrations oscillate as well as $[Ca^{2+}]_i$ and whether cytosolic Ca^{2+} stimulates or inhibits further release of Ca^{2+} from intracellular stores. The first model was formulated on the basis of the observation that in some cell types, elevated $[Ca^{2+}]_i$ inhibits the ability of IP_3 to release additional Ca^{2+} from internal stores (*2*). If this negative feedback has a sufficient time delay, it could explain Ca^{2+} oscillations that occur without IP_3 oscillations. A second model that postulates steady IP_3 elevation proposes that IP_3 merely transfers Ca^{2+} from the IP_3-sensitive internal stores to a separate IP_3-insensitive pool from which it is repetitively dumped by Ca^{2+}-induced Ca^{2+} release (*3*). This model is probably the most popular at present. Other models postulate that IP_3 concentrations do oscillate. For example, initial receptor stimulation of phosphatidylinositol-4,5-bisphosphate (PIP_2) hydrolysis might be self-limiting. This negative feedback would be mediated by diacylglycerol (DG) production and IP_3-mediated release of Ca^{2+}, which together would activate protein kinase C to phosphorylate the receptor or G protein and inhibit them, thus shutting off PIP_2 hydrolysis (model 3). Only when phosphatases had reversed the phosphorylation would another coordinated burst of IP_3, DG, and Ca^{2+} release be generated (*4*). A fourth model (*5*) proposes that phospholipase C can be stimulated not only by agonist but by cytosolic Ca^{2+}. Therefore an initial weak activation would self-amplify because Ca^{2+} released by IP_3 would further increase IP_3 production. This positive feedback would fail when the Ca^{2+} store was mostly depleted; only after a period of refilling could the burst of IP_3 and Ca^{2+} be repeated. This hypothesis, like model 2, predicts that an increase in $[Ca^{2+}]_i$ can release of stored Ca^{2+}, but in model 4 the positive feedback is mediated by IP_3, whereas in model 2 it is an inherent property of an IP_3-independent Ca^{2+} pool.

We have used the fibroblast cell line REF52 as a model system to study the mechanisms that generate $[Ca^{2+}]_i$ oscillations. This cell line was chosen because it gives unusually consistent oscillations (*6*): when appropriately stimulated by combined depolarization and treatment with mitogens or hormones such as vasopressin, essentially all the cells generate repetitive spikes in $[Ca^{2+}]_i$ (Fig. 1A). The amplitude and frequency of the spikes vary somewhat from cell to cell but in any one cell are remarkably consistent for hours. One set of experiments was directed at the question of whether Ca^{2+}, delivered by wounding or photolysis of a light-sensitive chelator, inhibits or stimulates further release from internal stores. A second series of experiments was to synchronize the $[Ca^{2+}]_i$ spikes in a population to see whether IP_3 fluctuates in parallel with $[Ca^{2+}]_i$. In a third group of experiments,

Howard Hughes Medical Institute M-047, University of California San Diego, La Jolla, CA 92093–0647.

*Present and permanent address: Department of Physiology, University of Maryland, 655 West Baltimore Street, Baltimore, MD 21201.
† To whom correspondence should be addressed.